

Detection of Abnormal Texture in Chest X-rays with Reduction of Ribs

Mira Park¹, Jesse S. Jin² and Laurence S. Wilson³

1. Department of Computer science and Software Engineering, The University of Melbourne, Victoria 3010, Australia

2. School of Information Technologies, Madsen Building F09, University of Sydney, NSW 2006, Australia

3. Telecommunications and Industrial Physics, CSIRO, PO Box 76, Epping NSW 1710, Australia

mirap@cs.mu.oz.au

Abstract

This paper presents a method to apply the general image retrieval algorithm on chest radiographs using *quasi*-Gabor filter. The lung field is extracted to limit the region to be processed using knowledge based lung field extraction method and the rib shadow is reduced to emphasis the lung texture.

Keywords: Chest X-ray, *quasi*_Gabor filter, Reduction of ribs, 2D-DFFT

1 Introduction

Medical image analysis is a complex task in which a human expert makes extensive use of the knowledge of anatomy and imaging techniques. Specially, the automatic segmentation of chest radiographs is challenging problem from a computer vision point of view. Because there are large anatomical variations from person to person and the most important problem is that radiographs are projection images and thus contain superimposed structures.

To interpret the chest radiographs, the radiologists often employ local properties like perceived intensity, uniformity, roughness, regularity, directionality, coarseness, smoothness and granulation [2]. For detection and characterization of these properties in radiological images, computer-aided diagnosis (CAD) schemes have been developed. CAD have usually included:

- Extraction of organs such as lung, heart, diaphragm, mediastinal, etc., using pixel classification [9][18], rule-based [8] and knowledge-based [14][7] methods.
- Detection of the rib cage using Hough transformation [13], a method based on modeling correspondence [14][15] and a method based on the gradient gray_level.
- Searching for isolated abnormal patterns [16][17][13][12][11][10]

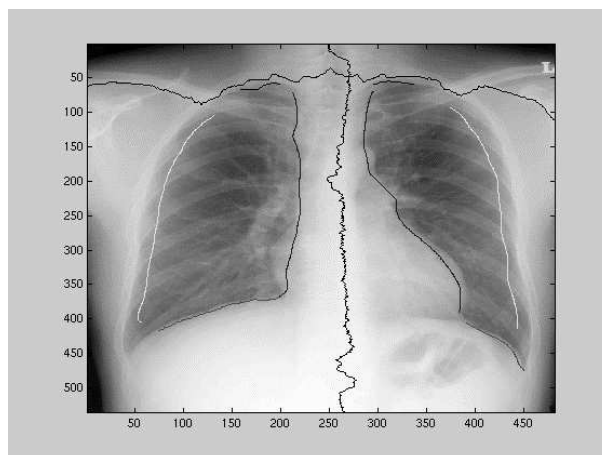


Figure 1 Extraction of lung field

However, all these proposed methods are designed for the chest radiographs since the local properties are often not clear and they are often superimposed with other organs, especially with the rib cage.

In this paper, we present a method to apply the general image retrieval algorithm on chest radiographs using *quasi*-Gabor filter developed by Park et al. [3][19]. It has already proved its high retrieval accuracy with low computational time. To apply this algorithm, we introduce a simple method to reduce the rib shadow.

The layout of this paper is as follows. In section 2, we will show the lung extraction module. In section 3, we will show the reduction of the rib shadow. In section 4, we will explain the *quasi*-Gabor filter and in section 5 we will detail our experiments, and finally in section 6, the conclusion of this paper will be presented.

2 Extraction of Lung Field

The lung field is extracted to limit the region to be processed. The knowledge based lung field extraction method, developed by Matthew et al. [14] and extended by Park [7], is applied to extract the lung field (see Figure 1). The system is a pixel-based feature extraction with a powerful, object-centered, knowledge-base inferencing system based on anatomical structures and relationships. An outline of the algorithm is as follows:

- Calculate edge points, with their associated gradient magnitude and phase (direction), eg., using Canny or LoG
- Apply magnitude and phase constraints, retaining only those points which satisfy the constrains

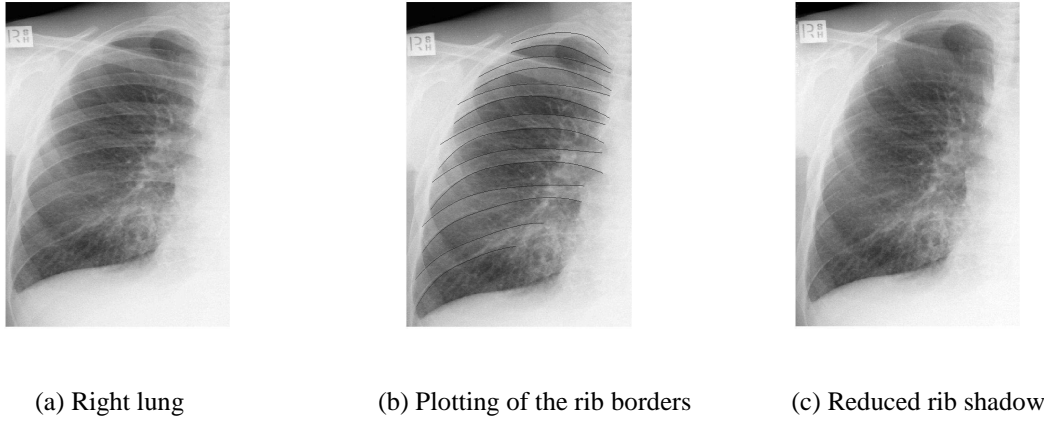


Figure 2 Reduction of ribs

- Form edge fragments from continuous sets of points
- Subdivide (split) edge fragments at points of high curvature
- Calculate all possible linkages of edge fragments to form candidates. A linkage can occur if the end points of the fragments are close enough, and the angle between them is within the orientation constraint range
- Discard all candidates which do not satisfy the length constraints
- Select the best candidate for matching to a frame on the basis of confidence scores.

3 Reduction of Rib shadow

To detect the rib border is not an easy task since there are different exposure levels of the different organs. However, it is worth applying one enhancement technique to the image causing some areas to be enhanced effectively while in other regions image quality is reduced [5]. The most efficient procedure is to filter the image with the Gaussian filter approximation before applying another operator such as Sobel and Robert [1]. We convolve one of the Sobel edge kernels to enhance the horizontal edges in the image and apply the edge detection algorithm to detect all the edges. From the edges, the rib border should be extracted using its characteristics such as length, start point, end point and gradient.

The rib borders are plotted on the original input image. There are two kinds of rib borders, which are a superior rib border and an inferior rib border (see Figure 2). The superior borders are represented by '0' and the inferior borders are represented by '1' in the original input image. We scan this image from left to right to plot the value along the same column. The difference between rib shadow and lung part without rib shadow is subtracted from the rib shadow since the rib shadow has higher density (1).

$$Av_of_n^{th}_rib = \left(\sum_{j=c_s}^{c_e} \sum_{i=st_{nj}}^{in_{nj}} f(i, j) \right) / (c_e - c_s) \quad (1)$$

$$Av_of_n^{th}_non_rib = \left(\sum_{j=c_s}^{c_e} \sum_{i=in_{nj}}^{su_{nj+1}} f(i, j) \right) / (c_e - c_s) \quad (2)$$

$$New_n^{th}_rib(i, j) = Old_n^{th}_rib(i, j) - ((1) - (2)) \quad (3)$$

$f(i, j)$ is the input image and c_s is the start of the rib border and c_e is the end of the rib border. su indicates the superior rib border and in indicates the inferior rib border. The Figure 2 (c) shows the lung field with the reduction of the rib shadow.

4 Detection of an Abnormal Nodule

The extracted lung field is divided into N 64x64 overlapping by 48 pixels subimages. This will resulting a more accurate image texture. The image feature vectors are extracted from each subimage using *quasi*-Gabor filter shown in Figure 3.

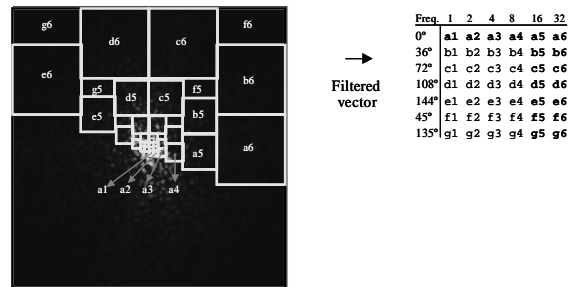


Figure 3 *quasi*-Gabor filter

The *quasi*-Gabor filter was developed by our team and we proved that the filter works very well with Brodatz image database [3][19]. We apply the filter in the frequency domain. Before the two dimensions DFFT (Discrete Fast Fourier Transform) is calculated we remove the mean value from the image because it tends to mean that the positive peaks of the waveforms are more likely to exceed the maximum level that can be represented. Then we use the Hamming windowing function to reduce DFFT leakage and the side lobes for improving DFFT results.

Next, the texture feature vector used to characterize each image in our experiments is derived with the *quasi*-Gabor

filter shown in Figure 3. First, the image is filtered through 42 channels by calculation of the energy for each block defined by a combination of one of 6 frequencies ($f = 1, 2, 4, 8, 16$ and 32) and one of 7 orientations ($\theta = 0^\circ, 36^\circ, 72^\circ, 108^\circ, 144^\circ, 45^\circ$ and 135°). The block size lays on $0^\circ, 36^\circ, 72^\circ, 108^\circ$ and 144° is $f^2 * 2^n / 2^7$ and the block size laid on 45° and 135° is half of the block size laid on other orientations when the size of the image is $2^n \times 2^n$. A single value, which becomes an entry in a 42-dimension texture feature vector, is then extracted from each block. We take the average value of the magnitude of the filtered image in each block. For using the *quasi*-Gabor filter, we do not need any convolution or multiplication of the image with the filter, so it is much faster than using Gabor filters or other filters.

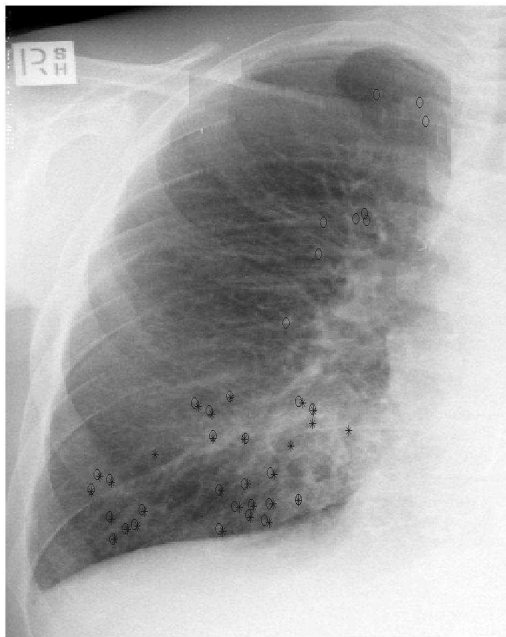


Figure 4 Detection PCP (Pneumocystis Carinii Pneumonia)

5 Performance Analysis

We extracted the lung field from the input radiograph and reduced the rib shadow. We then divided the lung field into N 64×64 overlapping by 48 pixels subimages. Our system extracted the image feature vectors from each subimage and classified them to identify the image as a normal texture class or as an abnormal class using k_{nn} classifier. Our lung texture database consisted of 2 classes and each class contains 20 normal lung textures and 20 abnormal lung textures. If the image belonged to the abnormal texture class, our system marked that area, which is 16×16 pixels, as an abnormal nodule. Figure 4 shows the small circle 'o' detected by our system and the star '*' detected by the radiologist for the abnormal (PCP: Pneumocystis Carinii Pneumonia) texture candidates.

6 Conclusion

In this paper, we applied the general image feature extraction method using *quasi*-Gabor filter on the radiographs with very low computation time even without any filter convolution, so the system is suitable for a real time system. We also showed a very simple method to reduce the rib shadow. The difficulty is that complete removal of the rib shadow may also remove the other textures, so we want to reduce the rib shadow without removing other texture that maybe abnormal interest. However we are still refining this system and current work involves manual conduction of the 'rib border plotting' step.

Further research will combine our method with the knowledge-based method to select the best candidates. Our system will also continue to diagnose the lung diseases based on all the information such as boundary, rib shadow and the location of the abnormal nodules of the lung.

7 Acknowledgement

We thank Dr. Bruce Doust in St. Vincent Hospital in Sydney for supplying all testing images and valuable medical verification advice.

8 References

- [1] John, S. D. and Martin D. F., Enhancement of Chest Radiographs with Gradient Operators, *IEEE transactions on medical imaging*, 7(2):109-116, 1988
- [2] Anne, M. F., Arivid, L., Michael, B., and Lothar, R. S., 8th Meeting of the ISMRM, www.uib.no/costb11/wg-madrid-nov-1999/amf_arivid_madrid99/ismrm2000.pdf, 2000
- [3] Park, M., Jin, J., and Wilson, L., Fast Content-Based Image Retrieval Using *quasi*-Gabor Filter and Reduction of Image Feature, 5th *IEEE Southwest Symposium on Image Analysis and Interpretation*, 178-182, 2002
- [4] Tetsuo S., Yoshio Y. and Naozo S., Construction of Structural Edge Map on Chest Radiograph Using Hough Transformation and Line connection, *Systems and Computers*, 26(6):71-78, 1995
- [5] Fredrick H. and Gerhard J., Model based segmentation of medical x-ray images, *Technical Report in Uni of Cape Town*, 1994
- [6] Zhanjun Y., Ardeshir G., and Laurens V., Automatic Detection of Rib Borders in Chest Radiographs, *IEEE Transactions on Medical Imaging*, 14(3):525-536, 1995
- [7] Park M., Wilson L., and Jin J., Automatic Extraction of Lung Boundaries by a Knowledge-Based Method, *Visual Information Processing*, 2:14-19, 2001
- [8] Bram G., and Bart M., Automatic segmentation of lung fields in chest Radiographs, *Medical Physics*, 27(10):2445-2455, 2000
- [9] Fu K., Chien Y., and Persoon E., *Computer Processing of Chest X-ray Images*, TR-EE 75-38, Purdue Uni, 335-354, 1975
- [10] Kunio D., Hever M., Shigehiko K., and Robertt M., Computer-aided diagnosis in radiology: Potential and pitfalls, *European Journal of Radiology*, 31:97-109, 1997
- [11] Chen X., Hasegawa J., and Toriwaki J., Quantitative diagnosis of pneumoconiosis based on recognition of small rounded opacities in chest x-ray images, *IEEE transactions on medical imaging*, 462-464, 1988

- [12] Matthew C., and Lawrence O., Automatic Tumor Segmentation using knowledge-based techniques, *IEEE transactions on medical imaging*, 17(2):187-201, 1998
- [13] Takeshi H., Hiroshi F., and Jing X., Development of automated detection system for lung nodules in chest radiographs, *IEEE transaction on medical imaging*, 71-74, 1997
- [14] Matthew B., Laurence W., Bruce D., Robert G., and Sun C., Knowledge-based method for segmentation and analysis of lung boundaries in chest X-ray images, *Computerized medical imaging and graphics*, 22:463-477, 1998
- [15] Wechsler H., and Sklansky J., Automatic detection of rib contours in chest radiographs, *International Joint Conference on Artificial Intelligence*, 688-695, 1975
- [16] Zhu X., Lee K., Levin D., Wong C., and Huang K., Temporal image database design for outcome analysis of lung nodule, *Computerized medical imaging and graphics*, 20(4):347-356, 1996
- [17] Tsuneo M., Hitoshi Y., Kunio D., and Maryellen G., Image feature analysis of false-positive diagnoses produced by automated detection of lung nodules, 587-597, 1991
- [18] Kim Y., Jeong K., and Lee K., A new algorithm for detection of lung boundary, *IEEE engineering in medicine & biology society*, 2770(6), 1989
- [19] Park, M., Jin, J., and Wilson, L., Hierarchical indexing images using weighted low dimensional texture feature, *15th IAPR International Conference on Vision Interface*, 39-44, 2002